

Cite this: DOI: 10.1039/c1cp20428a

www.rsc.org/pccp

On molecular chirality within naturally occurring secondary organic aerosol particles from the central Amazon Basin

Imee Su Martinez,^{†a} Mark D. Peterson,^{†a} Carlena J. Ebben,^a Patrick L. Hayes,^b Paulo Artaxo,^c Scot T. Martin^d and Franz M. Geiger^{*a}

Received 17th February 2011, Accepted 4th May 2011

DOI: 10.1039/c1cp20428a

In this perspectives article, we reflect upon the existence of chirality in atmospheric aerosol particles. We then show that organic particles collected at a field site in the central Amazon Basin under pristine background conditions during the wet and dry seasons consist of chiral secondary organic material. We show how the chiral response from the aerosol particles can be imaged directly without the need for sample dissolution, solvent extraction, or sample preconcentration. By comparing the chiral-response images with optical images, we show that chiral responses always originate from particles on the filter, but not all aerosol particles produce chiral signals. The intensity of the chiral signal produced by the size resolved particles strongly indicates the presence of chiral secondary organic material in the particle. Finally, we discuss the implications of our findings on chiral atmospheric aerosol particles in terms of climate-related properties and source apportionment.

Introduction

Plants emit monoterpene stereoisomers, *i.e.* chiral compounds that have the same chemical formula and atom connectivity but different spatial orientation of their atoms, at

concentrations that depend on geographic location^{1,2} and plant stresses.³ This “forest air of chirality”, as Stephanou calls it,⁴ was analyzed by Williams and co-workers and Ciccioli and co-workers, who reported ratios of 1 : 2 and 3 : 1 for the atmospherically important terpene stereoisomers (+)- to (–)- α -pinene in tropical forests and boreal forests, respectively.^{1,2} Given that α -pinene and related volatile organic compounds (VOCs) are important for the production of secondary organic aerosol (SOA),⁵ we consider in this perspective article the consequences for the molecular chirality impregnated into the aerosol particle phase produced from reactive chemistry in such air. We apply non-linear optical imaging to show that secondary organic aerosols collected at a field site in the central Amazon Basin under pristine background conditions during the wet and dry seasons are often chiral. The chiral

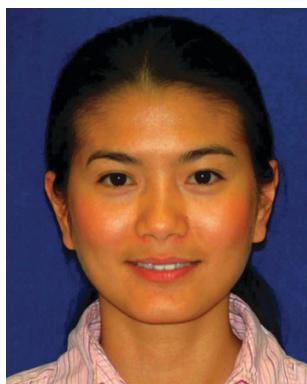
^a Department of Chemistry, Northwestern University, 2145 Sheridan Road, Evanston, IL 60208, USA

^b Department of Chemistry and Biochemistry, University of Colorado, and Cooperative Institute for Research in the Environmental Sciences, Boulder, CO 80309, USA

^c Institute of Physics, University of São Paulo, Rua do Matão, Travessa R, 187, 05508-090, São Paulo, Brazil

^d School of Engineering and Applied Sciences & Department of Earth and Planetary Sciences, Harvard University, 29 Oxford Street, Cambridge, MA 02138, USA

[†] ISM and MDP contributed equally to this work.



Imee Su Martinez

Imee Su Martinez is a graduate of the University of the Philippines who earned her PhD with Steve Baldelli at the University of Houston in 2010, where she worked on vibrational sum frequency spectroscopic studies of the surfaces of ionic liquids as a Welch Foundation Fellow. Her current work at Northwestern focuses on nonlinear optical studies of natural aerosol particles from boreal and tropical forests.



Mark D. Peterson

Mark David Peterson graduated from UC Irvine, where he worked with Sergey Nizkorodov, John Hemminger, Doug Tobias, and Benny Gerber on the atmospheric role of sea salt nanoparticles. He joined the Geiger research group in 2009 and developed nonlinear optical microscopy for imaging natural aerosol particles collected during field intensives.

responses always originate from particles on the filter, but not all particles produce chiral signals, which we quantify for highly size-resolved aerosol particles. Finally, we discuss the implications of molecular chirality in secondary organic aerosol particles and its possible utility to further advancing atmospheric science.

Chirality in nature

The rationale for reflecting upon the possibility of molecular chirality in atmospheric aerosol particles may be understood by first reviewing some salient points regarding chirality. Chirality is a property of a molecule or substance that is a common determinant of structure and function in nature.⁶⁻⁹ For instance, crystal growth in drug discovery depends critically on molecular chirality, and pharmacological properties (kinetics, dynamics, toxicology) often vary with chirality and chiral composition of drug polymorphs.¹⁰ The stereochemistry of natural products, which are prevalent in marine sponges, soil bacteria, and tropical plants, can be congested

enough to make their study an important focal point in synthetic organic chemistry.¹¹ In biological systems, the chirality of amino acids and nucleotides contributes to determining the function of peptides, proteins, RNA, and DNA.^{6,8}

The presence of chirality in a substance can be anticipated to have important effects on chemical reactivity and physical properties. This situation is very well known in polymer chemistry: chain end control¹² and the well-known nonlinearities in the yield of chiral reactions¹³ can produce biases in uneven mixtures of stereoisomer precursors that often result in the situation in which the stereogenic centers of one handedness dominate the molecular organization within an oligomer or a polymer. There are direct implications for chirality-dependent properties of the material formed: for instance, chirality in polymers determines the rigidity and the extent of crystallinity, molecular order, and long-range disorder of the polymer, which often determine the melting point and solubility of a polymer.^{14,15} While largely overlooked until now, this situation is directly relevant to tropospheric aerosol particles, as we will show below. Of particular relevance for this



Carlena J. Ebben

Carlena Jo Ebben is a graduate of Marquette University, where she worked with Scott Reid on the excitation and fluorescence spectroscopy of monohalo-carbenes. She joined Northwestern in 2009 and is working on chirality in cloud chemistry as an NSF Graduate Research Fellow in Franz Geiger's laboratories.



Patrick L. Hayes

Patrick Lewis Hayes is a graduate of Oberlin College who joined the Geiger group in 2004. He used vibrational sum frequency generation and second harmonic generation to study how anionic, cationic, and neutral adsorbates interact with oxide surfaces of biogeochemical and industrial importance. As an ARCS Fellow, Patrick built the kHz nonlinear optical microscope discussed in this perspectives article. Patrick is now a CIRES Postdoctoral Fellow with Jose Jimenez at the University of Colorado, Boulder, where he is studying the formation of secondary organic aerosols in urban air.



Paulo Artaxo

Paulo Artaxo is a professor of environmental physics at the University of São Paulo, Brazil. Artaxo studies atmospheric chemistry in the Amazon region, with a focus on aerosol physical and chemical properties. As one of the coordinators of the Large Scale Biosphere-Atmosphere Experiment in Amazonia, he helped to unveil the complex mechanisms that govern aerosol-cloud quantifying how aerosol particles influence carbon cycling and the radiation budget in

Amazonia. Paulo Artaxo is a Fellow of the AAAS, has published more than 200 scientific papers on the Amazonian aerosol particles, and holds more than 5400 citations.



Scot T. Martin

Scot Turnbull Martin received his BS at Georgetown University and his PhD in Physical Chemistry at Caltech as a DOE predoctoral Fellow with Michael Hoffmann. He arrived at Harvard in 2000 after completing a NOAA Postdoctoral Fellowship in Climate and Global Change at MIT with Mario Molina and serving on the faculty of the University of North Carolina. Martin, who is the Gordon McKay Professor of Environmental Chemistry, and his group recently completed

the Amazonian Aerosol Characterization Experiment (AMAZE-08), focusing on deciphering biological-climate connections and feedback mediated by chemistry in the central Amazonian Basin.

work is the role of chirality in biogenic volatile organic compounds (BVOCs) and their oxidation products that constitute the components of secondary organic aerosol (SOA) particles. Identifying and bridging this knowledge gap is important because BVOCs and SOA play prominent roles in the climate system.^{5,16,17}

Chirality in the troposphere

It is now understood that many BVOCs and their atmospheric oxidation products are chiral.¹⁸ Terpenes, which are BVOCs that are emitted in large quantities by trees to attract pollinators and repel herbivores, can exist in mirror image forms, *i.e.*, enantiomers.^{6,19,20} The molecular origin of this difference is rooted in the genetic evolution of cyclases,²¹ which convert isoprene into terpenes such as pinene, an important monoterpene representing 10–50% of the fraction of BVOCs.²² Upon reflecting on the fact that forests show a consistent enantiomeric preference in biogenic emissions of monoterpenes that depends on geographic location,^{1,2,4,21,23–25} and plant stresses,^{3,26} we are compelled to consider the consequences for the molecular chirality of aerosol particles. The rationale for this thought may be outlined as follows: oligomerization reactions between terpene oxidation products are important for forming the particle phase of atmospheric aerosols, specifically SOA.^{27–30} As discussed in the previous section, oligomerization reactions are known to be influenced by mechanisms involving chirality,^{12,13} often resulting in nonlinear biases between the chirality of macromolecules and the input of uneven mixtures of stereoisomer reactants. Consequently, we argue here that just as the input of uneven mixes of chiral feedstocks determines the properties of polymer in materials chemistry, asymmetric emission profiles of terpene emissions determine the chirality of secondary organic aerosol particles.

Relevant reaction pathways linking the emission of terpenes to the aerosol particle phase begin with terpene oxidation *via*, for instance, the gas phase ozonolysis of the terpenes, *i.e.* addition of ozone across a C=C double bond. Much is known about the mechanism associated with this process. In fact, the study of C=C double bond chemistry is a highly active area of

research that, one could argue, has led to more Nobel prizes than any other topic in the area of organic chemistry.^{31–39} Consider as an example the case of α -pinene, whose ozonolysis produces organic compounds such as pinonaldehyde and pinonic acid. These species have oxygen-bearing functional groups yet retain the four-membered ring.^{27,30,40,41} Recent work by Cataldo *et al.*,⁴² who subjected $\sim 1\%$ by volume concentrations of terpene stereoisomers in toluene to $\sim 10\%$ ozone content by weight, shows that chirality is preserved during this first step. We suggest that this may be the case for ppb and ppt level concentrations as well, where the reactions cascade beyond the monomeric ozonolysis product to yield oligomers. In fact, one possibility investigated in the field of SOA formation studies is that the monomeric terpene oxidation products undergo chemical reactions such as aldol addition to produce homo- and heterodimers and oligomers, whose progressively lower vapor pressures lead to the growth of the organic components of aerosol particles. A consequence of this general mechanism is that the initial stereoisomeric mix of the BVOC reactant—given by the (+)- to (–)- α -pinene ratio in our example—should determine the chiral balance of the particle. The chemical mechanism might be dominant for biogenically dominated regions, such as the Amazon Basin,⁴³ which is described in the following section.

The central Amazon Basin: an ideal natural laboratory to isolate biogenic SOA production

The Amazon Basin is the region of highest VOC emissions globally.^{44–46} During the wet season, the Amazon represents a pristine environment with nearly pure biogenic aerosol particles during much of the year,^{47–53} making it an ideal natural laboratory with well-characterized climatological and meteorological data⁴⁸ to isolate natural SOA production and thereby provides a baseline understanding against which to measure anthropogenic influences. Located on a ridge in the central Amazon Basin 60 km NNW of downtown Manaus is aerosol sampling tower TT34,⁴⁷ which is situated within a pristine terra firme rainforest in the Reserva Biologica do Cuieiras and managed by the Instituto Nacional de Pesquisas da Amazonia (INPA) and the Large-Scale Biosphere-Atmosphere Experiment in Amazonia (LBA). The forest canopy height near the tower varies between 30 and 35 m; the sampling height on the tower is 38.75 m. With respect to aerosol particles, site TT34 can be described as having wet, dry, and biomass burning seasons, although the biomass burning season at TT34 is greatly attenuated (*e.g.*, by a factor of 100 \times or more) compared to the “arc of fire” in the southern regions of the Amazon Basin.

Scanning electron microscopy (SEM) images of characteristic particle types collected during the recently completed Amazonian Aerosol Characterization Experiment (AMAZE-08) at TT34 using an impactor onto a substrate during the wet season of February and March 2008^{47,54} show that close to 90% of all detected particles consist of secondary organic aerosol (SOA) droplets that were formed by atmospheric oxidation and gas-to-particle conversion of biogenic volatile organic compounds and in which no other chemical components were detectable. The remaining portion of the particle phase



Franz M. Geiger

Franz Martin Geiger is a native of Berlin, Germany, where he received his Vordiplom from the Technische Universität. After his PhD with Janice Hicks at Georgetown University as a NASA Predoctoral Fellow in Earth Systems Sciences, and a NOAA Postdoctoral Fellowship in Climate and Global Change at MIT with Mario Molina, he arrived at Northwestern University in 2001, where he is currently the Irving M. Klotz Professor of Physical Chemistry. Geiger studies chirality in

cloud chemistry and physics with vibrational sum frequency generation and second harmonic generation applied to natural and synthetic aerosol particles of relevance to the climate system.

consists of secondary organic material mixed with sulfates and/or chlorides from regional or marine sources, primary biological aerosol particles, such as plant fragments or fungal spores, mineral dust particles consisting mostly of clay minerals from the Sahara desert, and pyrogenic carbon particles that exhibited characteristic agglomerate structures and originated from regional or African sources of biomass burning or fossil fuel combustion.

Chiral imaging of secondary organic aerosol particles

While much information is available regarding the origin, chemical composition, climate properties, and fate of the aerosol particles sampled during the wet season of February and March 2008,^{47,54} the molecular chirality of the particles was not investigated at that time. The small amount of SOA that is collected on the sampling filters or impactors makes it challenging to sample enough material for standard chiral analytics, which can require significant amounts of mass.^{7,55,56} The samples studied here were collected for multiple days during the 2008 wet season and contained as little as 80 micrograms of organic material, as determined by gravimetric analysis. Common sample preparation methods for chiral analysis of such small amounts of material involve dissolution of the particle phase followed by preconcentration prior to measurements or solid phase extraction.⁵⁵ Nonlinear optical techniques were applied in the study described herein to overcome these issues without the need for pre-concentration or sample destruction. Such methods take advantage of the very high sensitivity for chirality detection of second harmonic and vibrational sum frequency generation (SHG and SFG).⁵⁷

In the experiments, we use second harmonic and vibrational sum frequency generation (SHG^{58,59} and SFG^{60,61}), which are well-established nonlinear optical coherent methods that combine chemical specificity with structural sensitivity.⁶² The very high sensitivity of SHG and nonlinear optics towards

chirality⁵⁷ is manifested by a 100 to 10 000 fold increase of linear dichroism or circular dichroism effects when compared to non-coherent chirality measurements,^{7,57,63–66} and the molecular origins of this effect are discussed in the literature.⁵⁷ SHG and SFG allow for the study of chiral signatures from limited sample sizes and masses, such as those obtained through field sampling. Notably, the SHG response of chiral materials can be strong even when the experiments are carried out off electronic resonance.^{64,65,67,68} A milestone in SHG imaging^{67–78} was reached when Kriebel and Conboy imaged functionalized glass slides patterned with *R*- and *S*-binaphthol using chiral SHG microscopy.⁶⁸ Another milestone was reached when Hall and Simpson reported the direct observation of transient Ostwald crystallization ordering from racemic serine solutions using the same method, albeit with a laser scanning SHG microscope.⁷⁹

In general, the SHG response from chiral species is associated with the χ_{xyz} tensor element of the nonlinear susceptibility tensor $\chi^{(2)}$, which is unique to all chiral species.⁶⁰ Chiral SHG and SFG signals are bulk allowed, and the intensities scale with the square of the number of oscillators in a given bulk sample.⁸⁰ In the present work, SHG imaging is carried out using Kriebel and Conboy's + pioneering crossed-beam design,⁶⁸ which we adapted for a Ti:Sapphire amplifier laser system operating at a repetition rate of 1 kHz to produce 120 fs pulses at 800 nm (Fig. 1A). Fig. 1B shows the SHG response at 400 nm that is obtained from a plain glass slide following forty minutes of signal integration time and background subtraction, carried out by mismatching the arrival time of our two 120 fs probe pulses at the sample. The sample was imaged through an ultra-long working distance 10 \times objective (Zeiss). With a numerical aperture of 0.2, the maximum resolution for this objective is 1.2 microns. In the area of highest SHG intensity, the CCD detector (Princeton Instruments PIXIS 1024) records only around 50 counts per pixel over background in 40 minutes. The full width at half maximum (FWHM) of the horizontal SHG intensity profile is calculated from a Gaussian fit to be

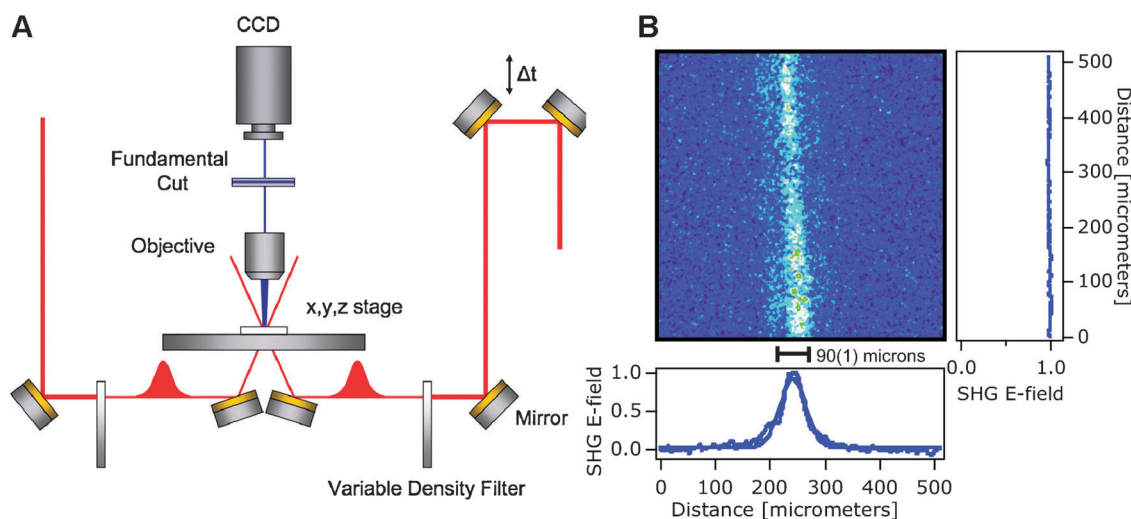


Fig. 1 (A) Crossed-beam SHG microscope for a kHz amplifier laser producing 120 fs pulses operating at incident angles of 20° from the surface normal. The SHG response is imaged at normal incidence. (B) Background subtracted SHG image obtained from a plain glass slide at 400 nm. The horizontal and vertical profiles of the SHG E-field, normalized to its highest value and referenced to zero, and Gaussian fit on the horizontal profile.

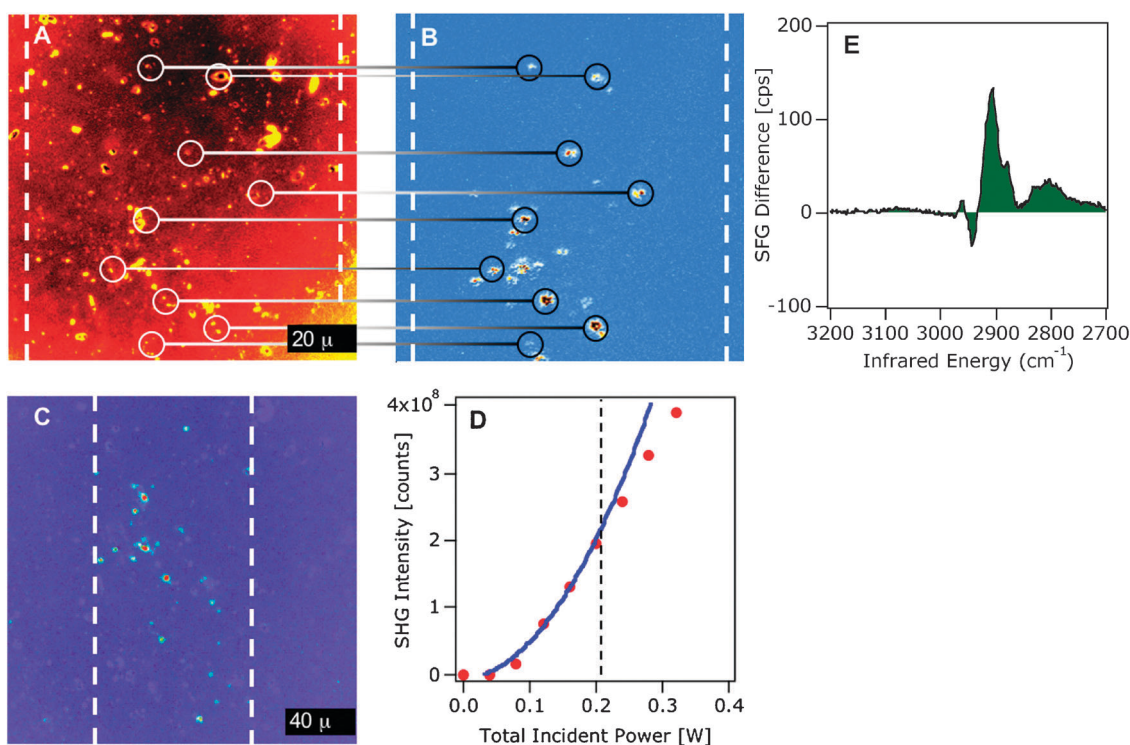


Fig. 2 (A) False-color optical and SHG image (B) from a glass slide that had been pressed against a Teflon filter containing aerosol particle material from the Amazon Basin. Circles connected by lines mark spatial correspondences between the two images. The vertical dashed lines mark the full width at half maximum of overlap of the fundamental probe light fields. (C) Zoomed out and slightly lower region of interest in the SHG image and field of view (white dashed lines) superimposed on its corresponding optical image. (D) Total SHG intensity as a function of incident power (filled circles) and power fit (line) yielding an exponent of 2.1 ± 0.1 for incident powers below the dashed vertical line. (E) Vibrational sum frequency generation difference spectrum obtained from the $p + 45p$ - and the $p - 45p$ -polarized SFG spectra of an aerosol particle-containing PM10 Teflon filter pressed against a fused silica window. Please see text for details.

90(1) micrometres. The low SHG signal intensities obtained from glass, which is achiral and possesses a low second-order susceptibility at the relevant wavelengths, indicate that it is an appropriate substrate for SHG imaging of secondary organic aerosol particles from Amazonia.

Fig. 2A and B show the false-color optical and background-subtracted SHG response, respectively, from a glass slide that had been pressed against a PM10-filter made of Teflon used for collecting aerosol particles over the entire size fraction below 10 micron at tower TT34 during the dry season month of July 2010. The sample was imaged through a $50\times$ ultra-long working distance objective (Zeiss). With a numerical aperture of 0.55, the maximum resolution for this objective is 440 nm at the SHG signal wavelength of 400 nm. The numerous sub-micron particles on the PM10-filter consisting mainly of secondary organic material, which are uniformly distributed across the filter, should dominate the chiral SHG response, provided that they are chiral. In contrast, primary biological aerosol particles in the supermicron size mode can be expected to contribute to the chiral SHG response when they are present in the cross sectional area of the probe beams. Fig. 2B shows that the aerosol particle material investigated here produced indeed a sizable SHG response. In fact, the SHG intensities from the chiral particles can be as high as 1000 counts over background in ten minutes. Fig. 2C, which shows a zoomed out and slightly lower region of interest superimposed on its corresponding optical image, indicates that

only a fraction of the particles are SHG active, a finding we will examine further below. Fig. 2D shows that the SHG response follows the expected quadratic power dependence for the appropriate energy range of fundamental probe light, after which departures from the quadratic response indicate the presence of processes other than SHG.

The strong SHG responses are attributable to chiral constituents in the aerosol particle material, as evidenced by their strong vibrational SFG linear dichroism responses, which we quantified independently in separate experiments carried out with a different amplifier laser system, detection optics, and laser laboratory. Following Shen's pioneering work⁸¹ as an independent test for chirality in these studies, Fig. 2E shows a pmp -polarized vibrational sum frequency generation (SFG) difference spectrum that was obtained from the $p + 45p$ - and the $p - 45p$ -polarized SFG spectra of aerosol particle containing Teflon filters pressed against fused silica windows. A hybrid scanning/broadband method pioneered by Esenturk and Walker⁸² ensured that each vibrational mode is accessed with the same incident IR power. To avoid optical damage, the incident pulse energies and foci were limited to 1 microjoules and 50 micrometres in diameter, respectively. Following our previously published procedures,⁸³ the SFG spectra were referenced to the SFG response from a gold substrate to account for the energy distribution in the infrared for each polarization combination and normalization to input power. The difference spectrum shown in Fig. 2E clearly shows strong

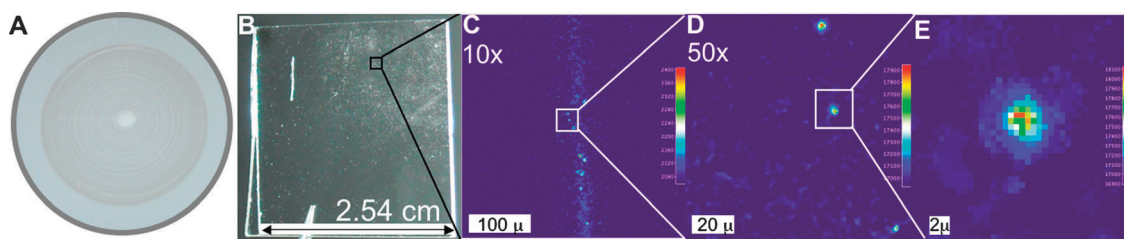


Fig. 3 Optical images of (A) MOUDI stage 3 collector plate (3.2–5.6 μm size range; aerodynamic diameter) and (B) a 1 \times 1 square inch glass slide onto which the filter had been pressed. SHG images obtained with a 10 \times (C) and 50 \times (D) objective from the area marked by the square. (E) View of the SHG image shown in (D), zoomed to the rectangular area.

vibrational chiral signal contributions, most of which occur in the aliphatic CH stretching region. This finding is consistent with a dominance of natural inputs into chemistry of the aerosol particles, as anthropogenic inputs are typically associated with aromatic CH stretches, which occur above 3000 cm^{-1} .^{84,85}

After confirming the chiral nature of the particle material on the collection filters, we proceeded to correlate their optical and SHG responses. Fig. 2A and B show that the chiral SHG responses always originate from material on the filter, but that not all optically visible material produces chiral SHG. In fact, as stated above, only a fraction of the particles are SHG active. In addition, we find that much of the chiral SHG response is due to sub-10-micron particles. Contributions from larger, primary biological particles, such as polysaccharide-rich bacteria, pollen, and plant debris—while clearly visible in the optical image—are minor on a number count basis in the SHG image. The SHG images presented in Fig. 2 suggest that this experiment can be carried out in the climate-relevant submicron size range. We therefore investigated highly size-resolved filter samples obtained during the 2008 wet season with a micro-orifice uniform-deposit impactor (MOUDI)⁸⁶ that is located at tower TT34. The 50% aerodynamic-diameter cutoff points for the stages of the MOUDI are, after an 18-micron cut-point inlet, 10.0, 5.6, 3.2, 1.8, 1.0, 0.6, 0.3, 0.2, and 0.1 μm , followed by an after-filter that collects the

remaining material with a nominal aerodynamic particle size of 5.6 μm . Fig. 3A shows the optical image of the 3.2–5.6 μm size range, and the concentric deposition pattern is clearly visible. Fig. 3B shows the photograph of a 1 \times 1 square inch glass slide onto which the filter shown in Fig. 3A had been pressed, and Fig. 3C shows an SHG image obtained within 20 minutes from the area marked by the square using our 10 \times objective. Multiple SHG-active spots are found and we examine three of them further by zooming into the region marked by the rectangle (Fig. 3D) with the 50 \times objective. The SHG intensity reaches values as high as 1000 counts over background in 120 min. The digital zoom displayed in Fig. 3E shows that the SHG response originates from a particle that has a diameter of about 4 μm , which falls within the relevant aerodynamic cutoff points of this particular sample.

Compared to the 3.2–5.6 μm size range, the 1.0–1.8 μm aerodynamic size range yields many more SHG active spots when compared to the optically visible spots. In the next smaller size range (0.33–0.56 μm) we find that the spots producing appreciable SHG intensities are markedly more isolated and there are less of them when compared to the optically visible spots. We conclude that the 1 to 1.8 μm size range contains the greatest relative proportion of particles exhibiting SHG activity—and thus chirality—when compared to the optically visible particles. This is quantified in Fig. 4A,

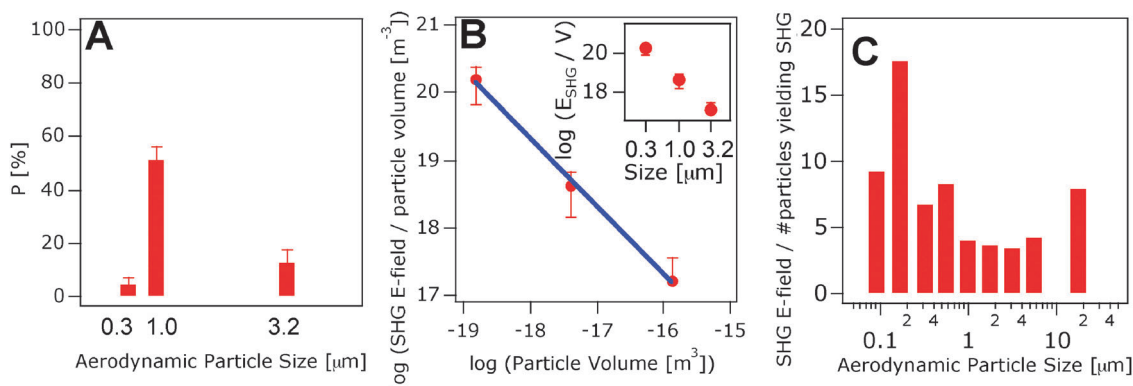


Fig. 4 (A) Percent of particles giving a chiral signal (P%) vs. optically visible particles as a function of aerodynamic particle size. (B) Background-corrected SHG E-field per individual particle divided by the volume of that particle averaged over all particles giving chiral signal in each filter stage examined as a function of average particle volume associated with that filter stage, calculated from the aerodynamic particle size. The straight line is a linear least-squares fit with a slope of 1.2 ± 0.8 and a slope of -1.01 ± 0.05 . The inset shows the logarithm of that SHG E-field as a function of the logarithm of the particle volume calculated from the aerodynamic particle size. All image data were obtained using 40 min signal integration time and a 10 \times objective. (C) SHG response normalized to the absolute number of optically visible particles that yield SHG as a function of aerodynamic particle size showing significant chiral contributions in the climate-relevant fine mode (<1 micron). An excess of 1000 particles was analyzed for this data set.

where we show the ratio of the number of SHG active spots to the number of optically visible spots for the three aerodynamic size ranges examined here. 178, 52, and 136 particles were optically observed for the 3.2–5.6 μm , 1.0–1.8 μm , and the 0.33–0.56 μm aerodynamic size ranges, respectively. We rationalize this observation as follows: the particles in the 0.33–0.56 μm size range have a longer atmospheric residence time than the supermicron particles⁴⁷ and are therefore subjected to more extensive chemical oxidation processing by OH radicals, water cycling, and related process collectively called ‘aging’ than larger particles. Given that a few percent of the long-lived particles show chiral signatures, we conclude that atmospheric aging can scramble chirality. As a result, the organic material in the aerosol particles may consist of oligomers each containing the same number of carbon atoms with opposite stereochemistry, either arranged randomly or in sequence along the oligomer, or it may consist of a racemic mix of oligomers that are each characterized by a net excess of chirality. Particles in the 1.0–1.8 μm size range have primarily biological cores and are coated by secondary organic material that is subjected to much less aging,⁴⁷ consistent with the observation that close to half of those particles show chiral signatures. Consistent with condensational growth,⁸⁷ AMAZE-08 also showed that the particles in the 3.2–5.6 μm size range have a smaller volume fraction of secondary organic material than those in the 1.0–1.8 μm size range,⁴⁷ which explains the low percentage of large particles giving the SHG signal. While only about 5% of the optically visible particles in the 0.33–0.56 μm size range produce a chiral signal, individual particles of this climate-relevant size range produce by far the strongest chiral response on a per-unit-volume basis when compared to the other aerodynamic sizes (Fig. 4B). This is shown for all nine stages of our MOUDI in Fig. 4C, which indicates that while not all particles in the fine mode are SHG active, they light up brightly, whereas many particles in the coarse mode are SHG active, but their SHG response is dim in comparison. The peak of this chirality distribution in the size range investigated here coincides with a peak in the particle surface-to-diameter distribution calculated from the number-diameter distribution of scanning mobility particle sizing, optical counting, and ultraviolet aerodynamic particle sizing.⁴⁷ This finding suggests the presence of a rich area of scientific research on the chirality of aerosol particles in the climate-relevant submicron size range, including surface-mediated reactions whose rate constants may depend on the molecular chirality of one terpene stereoisomer over another.⁸³

Summary and outlook

In this perspective article, we have reflected upon the possibility of chirality in atmospheric aerosol particles. Our findings indicate that while not all atmospheric particulate is expected to be chiral, an important class of atmospheric compounds, namely secondary organic aerosol particles, can contain chiral species and impart molecular chirality into atmospheric aerosol particles. One possible pathway for imparting molecular chirality into aerosol particles involves the mixing and condensation of chiral VOC oxidation products, which is analogous to mixing solutions of D- and L-configured sugars for demonstrating optical rotatory dispersion. Alternatively, aerosol particles that form *via* the oligomerization of terpene oxidation

products should produce chiral signals just like industrial materials do when they are formed from chiral and prochiral monomeric feedstocks.

While we have not yet determined what portion of a given particle contains chiral molecules and if that portion has an effect on the properties of the aerosol particle, we can suggest the following proposal for future directions in this exciting new arena of atmospheric chemistry: our finding of chirality in atmospheric aerosol particles of varying aerodynamic size ranges and ages leads us to contemplate that just as chirality can be important for determining the physical and chemical properties of molecules and materials, so can the chirality be important for determining aerosol particle properties. For instance, we expect tacticity, an important parameter for the melting points and dissolution rates of chiral polymers,¹⁵ to be important for aerosol particles in the atmosphere, where it could influence climate-relevant properties, including those that govern phase transitions and mixing. Given that the existence of chirality in atmospheric aerosol particles from natural pristine environments can now be readily benchmarked against the chirality in atmospheric aerosol particles from anthropogenic environments by using SHG microscopy, we can also test the potential use of chiral atmospheric markers as part of anthropogenic source apportionment procedures. For instance, burning refuse rich in industrial polymers may produce chiral signals in carbonaceous particulate matter that differ from those of carbonaceous particulate matter produced from burning forests. Likewise, chiral markers could contribute to current methods for distinguishing emissions from fossil and biofuel combustion. To this end, we are now quantifying chirality in aerosol particles *via* appropriately chosen terpene standards to obtain enantiomeric excess maps of atmospheric particulate matter, followed by developing statistical analysis methods for correlating chirality with particle origin and fate.

Acknowledgements

MDP acknowledges support from the Northwestern Initiative for Sustainability and Energy at Northwestern (ISEN). CJE gratefully acknowledges an NSF Graduate Research Fellowship. PLH acknowledges a scholarship from Achievement Rewards for College Scientists (ARCS), and Schlumberger Oilfield Chemical Products, LLC. PA acknowledges the support of FAPESP and CNPq for grants that funded part of this work. STM thanks the Office of Science (BES), U.S. Department of Energy, for support under grant No. DE-FG02-08ER64529. FMG thanks the National Science Foundation Atmospheric Chemistry division for support under grant no. NSF ATM-0533436 and gratefully acknowledges an EAGER grant from the Chemical Measurement and Imaging program in the Division of Chemistry under grant no. CHE-0937460. FMG also acknowledges support from an Irving M. Klotz professorship.

References

- 1 N. Yassaa, E. Brancaleoni, M. Frattoni and P. Ciccioli, *J. Chromatogr., A*, 2001, **915**, 185–197.
- 2 J. Williams, N. Yassaa and J. Lelieveld, *Atmos. Chem. Phys.*, 2007, **7**, 973–980.

- 3 A. V. Lavoie, M. Staudt, J. P. Schnitzler, D. Landais, F. Massol, A. Rocheteau, R. Rodriguez, I. Zimmer and S. Rambal, *Biogeosciences*, 2009, **6**, 1167–1180.
- 4 E. G. Stephanou, *Nature*, 2007, **446**, 991.
- 5 S. Solomon, D. Qin, M. Manning, Z. Chen, M. Marquis, K.B. Averyt, M. Tignor and H. L. Miller, *Climate Change 2007: The Physical Science Basis*, Cambridge University Press, Cambridge, UK, 2007.
- 6 J. March, *Advanced Organic Chemistry: Reactions, Mechanisms, and Structure*, Wiley & Sons, Inc., New York, 4th edn, 1992.
- 7 J. M. Hicks, *Chirality: Physical Chemistry*, Oxford University Press, Oxford, 2002.
- 8 D. Voet and J. G. Voet, *Biochemistry*, Wiley Text Books, New York, NY, 3rd edn, 2004.
- 9 K. Nakanishi and N. Harada, *Circular Dichroism Spectroscopy: Exciton Coupling in Organic Stereochemistry*, University Science Books, Mill Valley, CA, 1983.
- 10 D. Datta and D. J. W. Grant, *Nat. Rev. Drug Discovery*, 2004, **3**, 42–57.
- 11 E. L. Eliel, *Stereochemistry of Carbon Compounds*, McGraw-Hill, New York, 1962.
- 12 M. H. Chisholm, N. J. Patmore and Z. P. Zhou, *Chem. Commun.*, 2005, 127–129.
- 13 K. Soai, *Amplification of Chirality*, Springer Verlag, Heidelberg, 2010, vol. 284.
- 14 D. F. Shriver, P. W. Atkins and C. H. Langford, *Inorganic Chemistry*, Oxford University Press, Oxford, 1991.
- 15 A. F. Cotton, G. Wilkinson and P. L. Gaus, *Basic Inorganic Chemistry*, John Wiley & Sons, New York, 3rd edn, 1995.
- 16 J. H. Seinfeld and S. N. Pandis, *Atmospheric Chemistry and Physics: From Air Pollution to Climate Change*, John Wiley & Sons, New York, 1998, p. 1326.
- 17 B. J. Finlayson-Pitts and J. N. Pitts Jr., *Chemistry of the Upper and Lower Atmosphere*, Academic Press, New York, 2000.
- 18 R. Atkinson and J. Arey, *Chem. Rev.*, 2003, **103**, 4605–4638.
- 19 S. Hauptmann, *Organische Chemie*, 1st edn, VEB Harri Deutsch, Thun, Frankfurt am Main, 1985.
- 20 K. P. C. Vollhardt and N. E. Schore, *Organic Chemistry: Structure and Function*, W. H. Freeman Company, New York, 3rd edn, 1999.
- 21 M. A. Phillips, M. R. Wildung, D. C. Williams, D. C. Hyatt and R. Croteau, *Arch. Biochem. Biophys.*, 2003, **411**, 267–276.
- 22 M. Kanakidou, J. H. Seinfeld, S. N. Pandis, I. Barnes, F. J. Dentener, M. C. Facchini, R. Van Dingenen, B. Ervens, A. Nenes, C. J. Nielsen, E. Swietlicki, J. P. Putaud, Y. Balkanski, S. Fuzzi, J. Horth, G. K. Moortgat, R. Winterhalter, C. E. L. Myhre, K. Tsigaridis, E. Vignati, E. G. Stephanou and J. Wilson, *Atmos. Chem. Phys.*, 2005, **5**(4), 1053–1123.
- 23 M. A. Phillips, T. J. Savage and R. Croteau, *Arch. Biochem. Biophys.*, 1999, **372**, 197–204.
- 24 J. Bohlmann, C. L. Steele and R. Croteau, *J. Biol. Chem.*, 1997, **272**, 21784–21792.
- 25 J. L. Simonsen, *The Terpenes*, Cambridge University Press, Cambridge, 1957, vol. 2, pp. 105–191.
- 26 A. Guenther, S. Archer, J. P. Greenberg, P. Harley, D. Helmig, L. Klinger, L. Vierling, M. Wildermuth, P. R. Zimmerman and S. Zitzer, *Phys. Chem. Earth. Part B*, 1999, **24**, 659–667.
- 27 J. H. Kroll and J. H. Seinfeld, *Atmos. Environ.*, 2008, **42**, 3593–3624.
- 28 M. Kalberer, D. Paulsen, M. Sax, M. Steinbacher, J. Dommen, A. S. H. Prevot, R. Fisseha, E. Weingartner, V. Frankevich, R. Zenobi and U. Baltensperger, *Science*, 2004, **303**, 1659–1662.
- 29 K. J. Heaton, M. A. Dreyfus, S. Wang and M. V. Johnston, *Environ. Sci. Technol.*, 2007, **41**, 6129–6136.
- 30 K. J. Heaton, R. L. Slichter, P. G. Hatcher, W. A. Hall IV and M. V. Johnston, *Environ. Sci. Technol.*, 2009, **43**, 7797–7802.
- 31 K. Ziegler, E. Holzkamp, H. Breil and H. Martin, *Angew. Chem.*, 1955, **67**, 541–547.
- 32 G. Natta, P. Pino, P. Corradini, F. Danusso, E. Mantica, G. Mazzanti and G. Moraglio, *J. Am. Chem. Soc.*, 1955, **77**, 1708–1710.
- 33 T. M. Trnka and R. H. Grubbs, *Acc. Chem. Res.*, 2001, **34**, 18–29.
- 34 O. Diels, *Angew. Chem.*, 1948, **60**, 78–79.
- 35 K. Alder and G. Jacobs, *Chem. Ber.*, 1953, **86**, 1528–1539.
- 36 G. Wittig and U. Schollkopf, *Chem. Ber.*, 1954, **87**, 1318–1330.
- 37 R. F. Heck, *Org. React.*, 1982, **27**, 345–390.
- 38 R. Noyori and S. Hashiguchi, *Acc. Chem. Res.*, 1997, **30**, 97–102.
- 39 H. C. Kolb, M. S. Vannieuwenhze and K. B. Sharpless, *Chem. Rev.*, 1994, **94**, 2483–2547.
- 40 M. P. Tolocka, M. Jang, J. M. Ginter, F. J. Xoc, R. M. Kamens and M. V. Johnston, *Environ. Sci. Technol.*, 2004, **38**, 1428–1434.
- 41 K. S. Docherty, W. Wu, Y. B. Kim and P. J. Ziemann, *Environ. Sci. Technol.*, 2005, **39**, 4049–4059.
- 42 F. Cataldo, O. Ursini, E. Lilla and G. Angelini, *Ozone: Sci. Eng.*, 2010, **32**, 274–285.
- 43 S. T. Martin, M. O. Andreae, P. Artaxo, D. Baumgardner, G. Chen, A. H. Goldstein, A. Guenther, C. L. Heald, O. L. Mayol-Bracero, P. H. McMurry, T. Pauliquevis, U. Poeschl, K. A. Prather, G. C. Roberts, S. R. Saleska, M. A. S. Dias, D. V. Spracklen, E. Swietlicki and I. Trebs, *Rev. Geophys.*, 2010, **48**, RG2002.
- 44 A. Guenther, C. N. Hewitt, D. Erickson, R. Fall, C. Geron, T. Graedel, P. Harley, L. Klinger, M. Lerdau, W. A. McKay, T. Pierce, B. Scholes, R. Steinbrecher, R. Tallamraju, J. Taylor and P. Zimmerman, *J. Geophys. Res.*, [Atmos.], 1995, **100**, 8873–8892.
- 45 J. Kesselmeier, A. Guenther, T. Hoffmann, M. T. Piedade and J. Warnke, Natural volatile organic compound (VOC) emissions from plants and their roles in oxidant balance and particle formation, in *Amazonia and Global Change, Geophys. Monogr. Ser.*, vol. 186, ed. M. Keller and S. P. Dias *et al.*, 2009, pp. 183–206, AGU, Washington D. C.
- 46 M. Vrekoussis, F. Wittrock, A. Richter and J. P. Burrows, *Atmos. Chem. Phys.*, 2009, **9**, 4485–4504.
- 47 S. T. Martin, M. O. Andreae, D. Althausen, P. Artaxo, H. Baars, S. Borrmann, Q. Chen, D. K. Farmer, A. Guenther, S. S. Gunthe, J. L. Jimenez, T. Karl, K. Longo, A. Manzi, T. Pauliquevis, M. D. Petters, A. J. Prenni, U. Poeschl, L. V. Rizzo, J. Schneider, J. N. Smith, E. Swietlicki, J. Tota, J. Wang, A. Wiedensohler and S. R. Zorn, *Atmos. Chem. Phys.*, 2010, **10**, 11415–11438.
- 48 M. O. Andreae, P. Artaxo, C. Brandao, F. E. Carswell, P. Ciccioli, A. L. da Costa, A. D. Culf, J. L. Esteves, J. H. C. Gash, J. Grace, P. Kabat, J. Leslieveld, Y. Malhi, A. Manzi, F. X. Meixner, A. D. Nobre, C. Nobre, M. D. L. P. Ruivo, M. A. Silva-Dias, P. Stefani, R. Valentini, J. von Jouanne and M. J. Waterloo, *J. Geophys. Res.*, [Atmos.], 2002, **107**, 8066.
- 49 P. Artaxo, W. Maenhaut, H. Storms and R. Vangrieken, *J. Geophys. Res.*, [Atmos.], 1990, **95**(D10), 16971–16985.
- 50 M. O. Andreae, *Science*, 2007, **315**, 50–51.
- 51 M. Claeys, B. Graham, G. Vas, W. Wang, R. Vermeylen, V. Pashynska, J. Cafmeyer, P. Guyon, M. O. Andreae, P. Artaxo and W. Maenhaut, *Science*, 2004, **303**(5661), 1173–1176.
- 52 F. Gerab, P. Artaxo, R. Gillett and G. Ayers, *Nucl. Instrum. Methods Phys. Res., Sect. B*, 1998, **136**, 955–960.
- 53 S. T. Martin, M. O. Andreae, P. Artaxo, D. Baumgardner, Q. Chen, A. H. Goldstein, A. Guenther, C. L. Heald, O. L. Mayol-Bracero, P. H. McMurry, T. Pauliquevis, U. Poeschl, K. A. Prather, G. C. Roberts, S. R. Saleska, M. A. Silva-Dias, D. V. Spracklen, E. Swietlicki and I. Trebs, *Rev. Geophys.*, 2010, **48**, RG2002.
- 54 U. Poeschl, S. T. Martin, B. Sinha, Q. Chen, S. S. Gunthe, J. A. Huffman, S. Borrmann, D. K. Farmer, R. M. Garland, G. Helas, J. L. Jimenez, S. M. King, A. Manzi, E. Mikhailov, R. Pauliquevis, M. D. Petters, A. J. Prenni, P. Roldin, D. Rose, J. Schneider, H. Su, S. R. Zorn, P. A. Artaxo and M. O. Andreae, *Science*, 2010, **329**, 1513.
- 55 I. Salma, T. Meszaros, W. Maenhaut, E. Vass and Z. Majer, *Atmos. Chem. Phys.*, 2010, **10**, 1315–1327.
- 56 L. A. Nafie, T. A. Keiderling and P. J. Stephens, *J. Am. Chem. Soc.*, 1976, **98**, 2715–2723.
- 57 T. Petralli-Mallow, T. Maeda-Wong, J. D. Byers, H. I. Yee and J. M. Hicks, *J. Phys. Chem.*, 1993, **97**(7), 1383–1388.
- 58 R. M. Corn and D. A. Higgins, *Chem. Rev.*, 1994, **94**, 107.
- 59 K. B. Eisenthal, *Chem. Rev.*, 1996, **96**(4), 1343–1360.
- 60 Y. R. Shen, *The Principles of Nonlinear Optics*, John Wiley & Sons, New York, 1984.
- 61 G. L. Richmond, *Chem. Rev.*, 2002, **102**(8), 2693–2724.
- 62 F. M. Geiger, *Annu. Rev. Phys. Chem.*, 2009, **60**, 61–83.
- 63 B. J. Burke, A. J. Moad, M. A. Polizzi and G. J. Simpson, *J. Am. Chem. Soc.*, 2003, **125**, 9111–9115.
- 64 G. J. Simpson, *ChemPhysChem*, 2004, **5**, 1301–1310.

- 65 T. Verbiest, S. Van Elshocht, A. Persoons, C. Nuckols, K. E. Phillips and T. J. Katz, *Langmuir*, 2001, **17**, 4685–4687.
- 66 N. Ji and Y. R. Shen, *J. Am. Chem. Soc.*, 2004, **126**, 15008–15009.
- 67 R. D. Wampler, D. J. Kissick, C. J. Dehen, E. J. Gualtieri, J. L. Grey, H.-F. Wang, D. H. Thompson, J.-X. Cheng and G. J. Simpson, *J. Am. Chem. Soc.*, 2008, **130**, 14076–14077.
- 68 M. A. Kriech and J. C. Conboy, *J. Am. Chem. Soc.*, 2005, **127**, 2834–2835.
- 69 M. Nuriya, J. Jiang, B. Nemet, K. B. Eisenthal and R. Yuste, *Proc. Natl. Acad. Sci. U. S. A.*, 2006, **103**, 786–790.
- 70 A. J. Moad and G. J. Simpson, *J. Phys. Chem. A*, 2005, **109**, 1316–1323.
- 71 N. Ji, K. Zhang, H. Yang and Y.-R. Shen, *J. Am. Chem. Soc.*, 2006, **128**, 3482–3483.
- 72 Y. R. Shen, *Nonlinear Optical Spectroscopy of Molecular Chirality*, in *Trends and Perspectives in Modern Computational Science*, ed. G. Maroulis and T. Simos, Brill Academic Pub., The Netherlands, 2006, vol. 6, pp. 461–471.
- 73 R. D. Schaller, J. C. Johnson, K. R. Wilson, L. F. Lee, L. H. Haber and R. J. Saykally, *J. Phys. Chem. B*, 2002, **106**, 5143–5154.
- 74 K. Cimatu and S. Baldelli, *J. Am. Chem. Soc.*, 2008, **130**, 8030–8037.
- 75 P. Rechsteiner, J. Hulliger and M. Floersheimer, *Chem. Mater.*, 2000, **12**, 3296–3300.
- 76 A. C. Millard, L. Jin, J. P. Wuskell, D. M. Boudreau, A. Lewis and L. M. Loew, *J. Membr. Biol.*, 2005, **208**, 103–111.
- 77 R. Jin, J. Jureller, H. Y. Kim and N. F. Scherer, *J. Am. Chem. Soc.*, 2005, **127**, 12482–12483.
- 78 J. P. Long, B. S. Simpkins, D. J. Rowenhorst and P. E. Pehrsson, *Nano Lett.*, 2007, **7**, 831–836.
- 79 V. J. Hall and G. J. Simpson, *J. Am. Chem. Soc.*, 2010, **132**, 13598–13599.
- 80 M. A. Belkin, T. A. Kulakov, K. H. Ernst, L. Yan and Y. R. Shen, *Phys. Rev. Lett.*, 2000, **85**(21), 4474–4477.
- 81 M. Oh-e, H. Yokoyama, S. Yorozuya, K. Akagi, M. A. Belkin and Y. R. Shen, *Phys. Rev. Lett.*, 2004, **93**, 26.
- 82 O. Esenturk and R. A. Walker, *J. Phys. Chem. B*, 2004, **108**(30), 10631–10635.
- 83 G. Y. Stokes, F. C. Boman, J. M. Gibbs-Davis, B. R. Stepp, A. Condie, S. T. Nguyen and F. M. Geiger, *J. Am. Chem. Soc.*, 2007, **129**, 7492–7493.
- 84 G. Herzberg and R. E. Krieger, *Molecular Spectra and Molecular Structure. Vol. I. Spectra of Diatomic Molecules*, Malabar, FL, 1989.
- 85 M. Hesse, H. Meier and B. Zeeh, *Spektroskopische Methoden in der Organischen Chemie*, ed. G. Thieme, Stuttgart, New York, 4th edn, 1991.
- 86 V. A. Marple, K. L. Rubow and S. M. Behm, *Aerosol Sci. Technol.*, 1991, **14**(4), 434–446.
- 87 S. F. Maria, L. M. Russell, M. K. Gilles and S. C. B. Myneni, *Science*, 2004, **306**(5703), 1921–1924.